Chapter 5
ACC and Vaterite as Intermediates in the Solution-Based Crystallization of $CaCO_3$

Juan Diego Rodriguez-Blanco, Karina K. Sand, and Liane G. Benning

5.1 Introduction

Calcium carbonate minerals are ubiquitous on Earth where they play a key role in many marine and terrestrial biomineralization processes (e.g., see also Chap. 9 by Falini and Fermani in this book). Their ubiquitous nature makes them key players in controlling a large part of the global carbon cycle. At ambient temperatures, they very often crystallize from solution via two intermediate phases: amorphous calcium carbonate (ACC) and vaterite.

ACC is a poorly ordered material (50–500 nm) (Rodriguez-Blanco et al. 2008) that in its pure form (no other cations but Ca^{2+} present at formation) consist of a Ca-rich framework with 1-nm diameter interconnected pores that contain water and carbonate ions (Goodwin et al. 2010). In recent years, ACC has been shown to

---

J.D. Rodriguez-Blanco (✉)
Department of Geology, Trinity College Dublin, Dublin 2, Ireland

NanoScience Center, Department of Chemistry, University of Copenhagen,
Copenhagen, Denmark
e-mail: jblanco@nano.ku.dk; j.d.rodriguez-blanco@tcd.ie

K.K. Sand
NanoScience Center, Department of Chemistry, University of Copenhagen,
Copenhagen, Denmark

Physical Sciences Division, Pacific Northwest National Laboratories, Richland, WA, USA

L.G. Benning
German Research Center for Geosciences, GFZ, Interface Geochemistry Section,
14473 Potsdam, Germany

Department of Earth Sciences, Free University of Berlin, 12249 Berlin, Germany

School of Earth and Environment, University of Leeds, Leeds LS2 9JT, UK

A.E.S. Van Driessche et al. (eds.), *New Perspectives on Mineral Nucleation and Growth*,
DOI 10.1007/978-3-319-45669-0_5

exhibit a complex chemical make up with variable hydration states linked to its “structure” at the short-range scale (Radha et al. 2010). Laboratory-synthesized ACC is often highly hydrated (<1.6 mols of water per mole of $CaCO_3$) and thermodynamically unstable. In the absence of additives, and when equilibrated with the solution, ACC transforms extremely fast (<2 min at 25° C; Rodriguez-Blanco et al. 2011) to crystalline $CaCO_3$ polymorphs. This transformation can take multiple, and sometimes complex, pathways that are dependent on the physico-chemical environment. Conversely, biogenic ACC is often initially hydrated, but during aging of ACC-rich biominerals (e.g., spine spicules; Gong et al. 2012), it slowly dehydrates concomitantly increasing its short-range order. In contrast to synthetic ACC, biogenic ACC can persist for days in the animal (Gong et al. 2012) and months when extracted and stored in dry conditions (Politi et al. 2008; Gong et al. 2012). Similarly carbonate concretions that are released by certain earthworm species (e.g., Brinza et al. 2014; Hodson et al. 2015) contain ACC stabilized for very long time periods, yet the reason of this stabilization is still unknown.

The main problem is the fact that the degree of ordering, hydration, particle size, and crystallization of ACC are largely controlled by its origin and conditions of formation. These include a number of factors like temperature, pH, and concentration of foreign ions in solution (e.g., Mg^{2+}, SO_4^{2-}, PO_4^{3-}, organics, etc.). For example, pure ACC usually transforms to calcite via a vaterite intermediate at low temperatures (<30 °C) and via aragonite at higher temperatures (>60 °C). However, small variations in initial pH of the aqueous solution (Tobler et al. 2016) or the presence of divalent ions (e.g., Mg^{2+}, Sr^{2+}) or organics (e.g., aspartic acid, glutamic acid, citric acid, etc.) can dramatically affect the crystallization rates and pathways of ACC, also resulting in the incorporation of variable amounts of these ions in the ACC structure (e.g., Wang et al. 2009; Rodriguez-Blanco et al. 2014; Tobler et al. 2015).

So far most studies focused on the formation and crystallization of ACC in abiotic systems (e.g., Ogino et al. 1987; Faatz et al. 2004; Radha et al. 2010; Rodriguez-Blanco et al. 2011). However, many biomineralization processes that ultimately lead to calcite or aragonite as the prime calcium carbonate phase occur within a biological membrane where (1) the activity of water is lower compared to a “pure” aqueous solution and (2) there is a high concentration of organic macromolecules, which fulfill a wide variety of functions (e.g., energy storage, structural protection, insulation). It is well known that the two most abundant $CaCO_3$ biominerals (i.e., calcite and aragonite) have remarkable morphologies, defined crystallographic orientations, and extraordinary functional properties (Dove et al. 2003). However, many biomineralizing organisms use the ACC to crystalline calcium carbonate pathway to control particle shape, crystallographic orientation, and crystalline polymorph during the formation of their shells, spines, etc. One of the best-known examples of ACC produced in biomineralization processes is found in sea urchins, which produce elongated single crystals of calcite with the c-axis aligned parallel to the length of the spicules. However, important for this chapter is the fact that they do this by controlling the deposition and crystallization of ACC within a biological membrane (Beniash et al. 1997). Similarly, ACC has also been found in the intestinal lumen of gilt-head sea bream *Sparus aurata* (Foran et al.

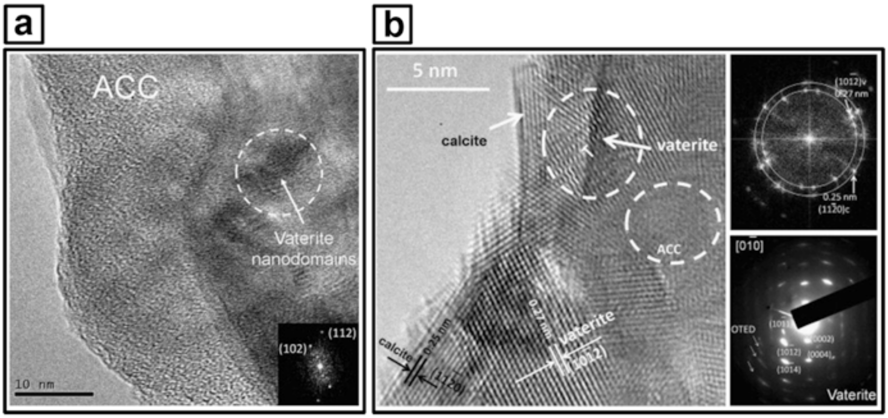

Fig. 5.1 $CaCO_3$ biomineralization produced by earthworms. (**a**) spherulitic deposit showing an ACC region with some minor contributions of crystalline phases in the form of small clusters (*inset circle*: selected area electron diffraction diagram of a vaterite single crystal represented along the [−2 0 1] zone axis). (**b**) Area of the spherulite showing vaterite nanocrystals partially transformed to calcite (calcite domains tend to be oriented with lattice planes parallel to the spherulite's edge and the regions between vaterite domains are separated by amorphous areas). The selected area electron diffraction diagram shown in the *inset* at the *bottom* of this figure corresponds to a single crystal of vaterite viewed along [0−1 0] showing these features. The *top inset* shows the fast Fourier transform analysis of the whole micrograph revealing a powderlike pattern (See more details in Gago-Duport et al. 2008)

2013), in some plants as the main component of cystoliths (Gal et al. 2012) and in earthworms' calciferous glands (Gago-Duport et al. 2008; Hodson et al. 2015). On the other hand, vaterite formed from ACC is often unstable. Nevertheless, although vaterite is rarely preserved in geologic settings (compared to calcite and aragonite), it is more common as a product of biomineralization. For example, vaterite has been found in earthworms calciferous glands (e.g., Fig. 5.1; Gago-Duport et al. 2008; Brinza et al. 2014), otoliths (Wehrmeister et al. 2011), lackluster pearls (Qiao et al. 2007), or spicules of tropical ascidian (Lowenstam and Abbott 1975; Kabalah-Amitai et al. 2013) or in aberrant growth of mollusk shells repaired after an injury (Isaure et al. 2010).

In recent years, these unusual biomineralization processes have attracted considerable interest because of their potential to be replicated, and controlled, in the laboratory. By using different methods (e.g., molecular templates, tailored self-assembly mechanisms), it could be possible to manufacture industrial $CaCO_3$ nanoparticles with specific sizes and shapes that would result in many applications for material sciences, biomedical research, food, agriculture, etc. For example, the crystallization processes of carbonates have great potential for incorporation of proteins or pharmaceutical compounds (e.g., insulin; Fujiwara et al. 2010), opening the door to simple and cost-effective methods for storage and targeted drug-delivery applications (e.g., vaterite nanocapsules; Parakhonskiy et al. 2012). All these applications require an understanding of the fundamental factors controlling the structures and crystallization pathways of calcium carbonates during the earliest stages of crystallization, i.e., during the formation of metastable phases like ACC and vaterite. However, the instability and rapid transformation tendency of ACC (e.g., in the pure system, seconds–minutes) can make an in depth characterization very difficult. Furthermore, to follow the rapid transformation reactions to crystalline carbonate, especially when they proceed via short-lived intermediate phases (e.g., vaterite, aragonite) is also not trivial. However, over the last few years, new experimental and characterization approaches have been developed, combining classical characterization techniques with methods that allow in situ and real-time monitoring of the reactions (e.g., time-resolved synchrotron-based scattering and diffraction, in situ liquid cell high-resolution microscopy, time-resolved spectrophotometry, in situ titrations, and ultracentrifugation; Rodriguez-Blanco et al. 2011; Nielsen et al. 2014; see also Chap. 18 by Nielsen and De Yoreo in this book; Burke et al. 2015; Tobler et al. 2015). These techniques have provided very useful data to attain the mechanisms and quantify the kinetics of ACC crystallization in abiotic systems. In addition, they provided a detailed understanding of how calcium carbonate phases form during biomineralization processes when the system moves from ACC toward thermodynamic equilibrium with calcite.

5.2 Mechanisms of Crystallization of Vaterite and Calcite from ACC

Since the 1970s, vaterite was assumed to be a possible precursor phase during the formation of $CaCO_3$ in sediments (Rowlands and Webster 1971). This assertion was confirmed by experimental observations showing that vaterite forms prior to calcite, at moderate or high supersaturations (Ogino et al. 1987). In addition, now it is well known that natural ACC crystallizes to vaterite in solution. Yet, the debate about the mechanisms of crystallization of vaterite from ACC, also linked to the complexity of determining its precise mineral structure (Kabalah-Amitai et al. 2013) and understanding its thermodynamic stability (Wang and Becker 2012), is in part still ongoing.

Just recently, cryo-TEM studies revealed that the transformation from ACC to vaterite can occur through a direct solid-state transformation. Crystalline domains have been observed after the aggregation of ACC nanoparticles into larger particles, and this was coupled with dehydration of the precursor phase. This combined aggregation and crystallization of ACC is considered to result in the development of randomly oriented crystalline domains that forms the typically observed spherical aggregates (Pouget et al. 2009; Pouget et al. 2010).

However, most studies consider that the ACC–vaterite transformation is a solution-mediated transformation mechanism that consists of ACC dissolution coupled to vaterite crystallization (e.g., Shen et al. 2006). Over the last decade, a number of nucleation and growth studies have taken advantage of the developments in synchrotron-based scattering and diffraction technologies that allow quantifying such reactions in situ, and real time, for more realistic conditions. Such methods have been previously tested on other minerals systems like amorphous silica (Tobler et al 2009; Tobler and Benning 2011), iron compounds (e.g., sulfides: Cahill et al. 2000; oxides: Davidson et al. 2008; Vu et al. 2010; Brinza et al. 2015) and sulfates (Ahmed et al. 2010). All these studies followed the formation and transformation of phases in situ and in real time based on changes in diffraction or scattering properties of the solids that were reacting in the aqueous solutions. Recently, this approach was also applied to the crystallization of ACC (Fig. 5.2), and this was possible at very high temporal resolutions (1 s/scan), over realistic time spans (secs-10's of secs), and for a wide range of supersaturation, temperature, pH, and additive concentrations. These studies provided new data on the nucleation and growth of $CaCO_3$ phases, i.e., the evolution of their particle sizes and shapes as well as the changes in short- or long-range order (crystallinity) of solids that are in continual contact with the reacting solutions. We crystallized (Bots et al. 2012; Rodriguez-Blanco et al. 2012) vaterite and calcite from solution via ACC from mixtures of highly concentrated (1 M) Na_2CO_3 and $CaCl_2$ solutions. They followed the reactions at 1–30 s time frames using small- and wide-angle X-ray scattering (SAXS/WAXS) and showed that the polymorph selection during the crystallization of ACC was highly pH-dependent but that other additives also changed the reactions dramatically. While a neutral (<7) starting pH during mixing promoted the direct transformation of ACC into calcite, when ACC formed from a solution with a basic initial pH (<11.5), the transformation to calcite occurred via metastable vaterite (Fig. 5.2). The early stages of crystallization of vaterite from ACC at basic initial pH (<11.5) and starting saturation index of $SI = 4.2$ started with the rapid breakdown of ACC and was followed by an equally rapid nucleation and spherulitic growth of vaterite (<2 min).

Spherulitic growth is a fast growth process that proceeds via the continuous nucleation of new nanoparticles on the surface of an already existing particle (core) via non-crystallographic branching. This nucleation-controlled growth process is usually termed "growth front nucleation" or "secondary nucleation" (Gránásy et al. 2005; Shtukenberg et al. 2012). In this process, there is no structural relationship between the newly nucleated particles and the already existing ones. This results in the formation of micrometer-sized spherulites that consist of aggregates of monodisperse nanoparticulate crystallites. Spherulitic morphologies have been categorized in two types: spheres (category 1) and dumbbells (category 2). This morphological variability is related to an orientation-dependent grain boundary energy change. Andreassen et al. (2010) experimentally demonstrated that spherulitic growth of vaterite directly from solution (i.e., not via an ACC precursor) requires a high crystallization driving force (i.e., $SI > 2–3$) to promote fast crystallization rates, leading to the formation of spherical nanocrystal aggregates. Spherical aggregates of vaterite crystallized via ACC have often been observed (Fig. 5.2), yet morphological evidence on its own is not satisfactory to provide definitive confirmation for spherulitic growth. Such evidence was derived from the change in saturation index of vaterite in the aqueous solutions at equilibrium with respect to ACC which was $SI = 1.4$ (Bots et al. 2012). However, SAXS/WAXS data revealed a

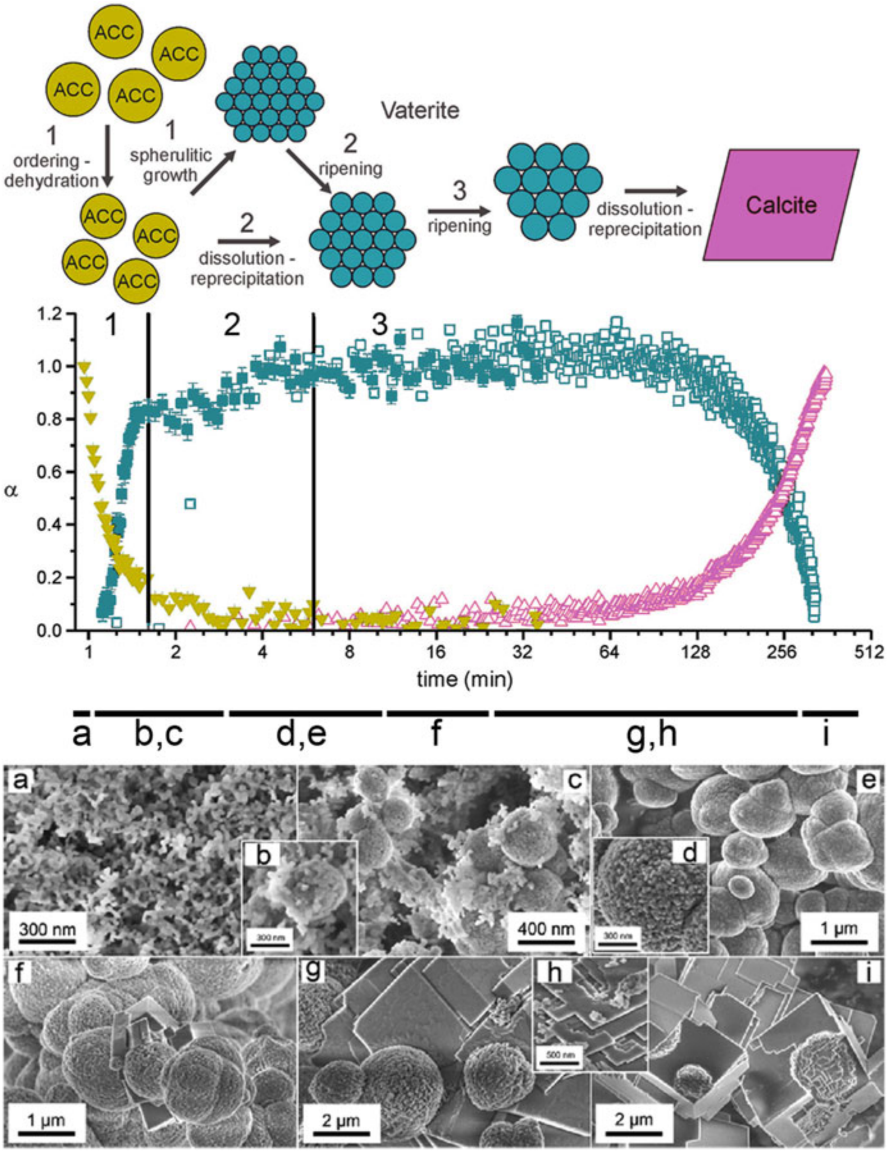

Fig. 5.2 *Top* diagram shows an schematic representation of the proposed multistage ACC → vaterite → calcite crystallization pathway (*top*) with the underlying combined reaction progress, α_{ACC}, $\alpha_{\mathrm{vaterite}}$, and $\alpha_{\mathrm{calcite}}$, for the full crystallization reaction in the pure ACC system (the *green triangles* and *full black squares* represent the ACC and vaterite from Bots et al. (2012) and the *open squares* and *red triangles* represent the vaterite and calcite from Rodriguez-Blanco et al. 2011); stages 1, 2, and 3 of the reaction mechanism are labeled on the figure. FEG-SEM images show the solid phases that form during these stages of the crystallization process. Pictures on the *top* correspond to the ACC → vaterite transformation: amorphous calcium carbonate (ACC) (**a**), ACC and vaterite nanoaggregates (**b**, **c**), and vaterite nanoaggregates (**d**, **e**). Pictures at the *bottom* correspond to vaterite → calcite transformation: vaterite nanoaggregates and first calcite crystals (**f**), calcite crystals attached to vaterite spheres with the development of growth steps on the calcite surface (**g**), calcite growth steps and vaterite nanoparticulate subunits, (**h**) and calcite crystals with vaterite casts (**i**) (after Rodriguez-Blanco et al. 2011)

fast breakdown of minor amounts of ACC prior to the crystallization of vaterite, resulting in a rapid increase in supersaturation, providing the high crystallization driving force needed for spherulitic growth. In addition, these data showed that the ACC–vaterite reaction proceeded via a continual dissolution of ACC and growth of vaterite. ACC that started off as ~35 nm particles was present until virtually all the vaterite had formed, keeping the supersaturation at a sufficiently high level to allow continuous vaterite nucleation. Furthermore, the SAXS/WAXS data clearly showed extremely rapid crystallization rates of vaterite, which are typical during a nucleation-controlled growth mechanism like spherulitic growth. Overall, the high level of supersaturation due to the breakdown of ACC promoted very rapid crystallization kinetics. The complete crystallization of vaterite occurred in <2 min and the average crystallite/particle sizes for the vaterite started off at ~10 nm, consistent with a nucleation dominated particle formation reaction with very little or no surface growth. At the end of the reaction, the particles reached a maximum size of ~40–60 nm, depending if sulfate was present in the aqueous solution or not.

Although spherulitic growth has been observed in other systems (i.e, polymers supercooled from a molten state or viscous magmas; Shtukenberg et al. 2012 and references therein), in carbonates it is promoted when the difference in solubility between the amorphous precursor phase and any crystalline phase is largest. Besides vaterite, other carbonates can also grow by a spherulitic mechanism: calcite (Rodriguez-Blanco et al. 2012), aragonite (Sand et al. 2012), monohydrocalcite (Rodriguez-Blanco et al. 2014), dolomite (Rodriguez-Blanco et al. 2015), or even REE-bearing carbonates like tengerite, kozoite, or hydroxylbastnasite (Vallina et al. 2014; Vallina et al. 2015) (Fig. 5.3). Interestingly, spherulitic morphologies are not just a vagary of experimental systems as they have also been observed in natural biogenic carbonates like corals that crystallize aragonite (Holcomb et al. 2009) or in microbial systems that produce proto-dolomite/dolomite (Warthmann et al. 2000; Sánchez-Román et al. 2011). Again, these reactions proceed when locally very high supersaturations are reached. The fact that Mg^{2+} and REE^{3+} ions play an important role in the process is primarily linked to their high dehydration energies (Fedorov et al. 2002; Di Tommaso and De Leeuw 2010). When they are present within the porous structure of the precursor phase, they retard its dehydration, thereby reducing the rate of dissolution and decreasing its overall solubility. As a result, in abiotic systems, high temperatures are sometimes required to promote the breakdown of the amorphous precursor phase and the fast increase in supersaturation levels during the crystallization process.

Above we primarily focused our discussions on how ACC transforms to vaterite. We also showed that once metastable vaterite has fully formed, it starts transforming into calcite. This process is temperature-dependent. We (Rodriguez-Blanco et al. 2011) derived the rates and energetics for the vaterite–calcite transformation reaction from 7.5 to 25° C, conditions which are relevant for both biomineralization and industrial calcium carbonate formation reactions. We found that the vaterite–calcite transformation is a surface-controlled process that occurs at much slower rates (e.g., 6 h at 25°°C) compared to the formation of vaterite via spherulitic growth (minutes). We also showed that the surface area of the newly forming calcite

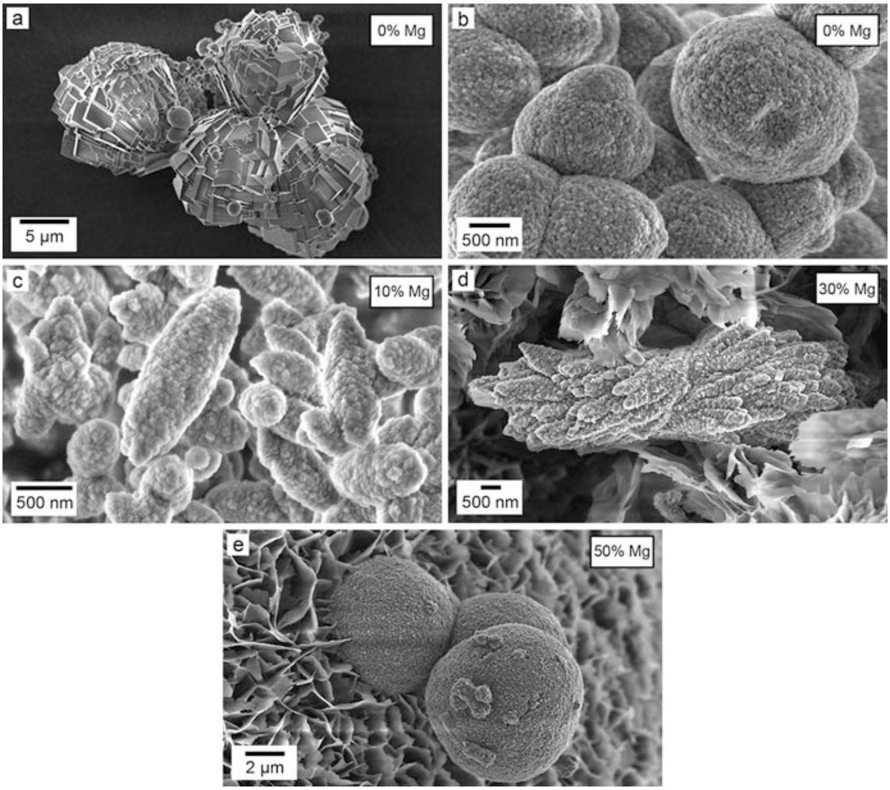

Fig. 5.3 Spherulitic morphologies of the first crystalline products obtained after the breakdown of pure or Mg-bearing ACC: (**a**) calcite, (**b**) vaterite, (**c**) Mg-calcite, (**d**) monohydrocalcite, (**e**) dolomite. Hydromagnesite ($Mg_5(CO_3)_4(OH)_2 \cdot 4H_2O$) is also a seen in the background of images (**d**) and (**e**) as it is usually a secondary product that forms during the crystallization of monohydrocalcite and dolomite. % Mg shown in each picture corresponds to $[Mg^{2+}]_{aq}/[Ca^{2+}]_{aq} \cdot 100$ in solution before the formation of ACC

controls the crystallization rate. This reaction proceeds via the slow dissolution of vaterite, followed by the gradual increase in its porosity and the release of calcium and carbonate ions into the solution. This leads to a surface-mediated dissolution–reprecipitation and growth of calcite crystals (Fig. 5.2f–h). This calcite consists of crystals with rhombohedral morphologies because during the vaterite–calcite transformation, the aqueous solution is in equilibrium with respect to vaterite, so the saturation index of calcite ($SI = 0.57$) is too low to favor spherulitic growth.

Although calcite is sometimes a product of the recrystallization of vaterite, the formation of ACC at neutral ($\sim$7) starting pH and at high supersaturations can also result in the primary crystallization of spherulitic calcite (Beck and Andreassen 2010; Rodriguez-Blanco et al. 2012). Again, this is driven by the large enough difference between the solubility of ACC and calcite to provide the high supersaturation ($SI > 2$–3) needed for spherulitic growth. Spherulitic calcite is not so common in nature compared to spherulitic vaterite, but there are examples that show that these morphologies may originate during biomineralization processes. Many species of earthworm secrete granules of calcium carbonate that are formed within the earthworm's calciferous glands. These granules are mainly made of calcite but also contain remnant ACC, vaterite, and aragonite (Canti and Piearce 2003; Briones et al. 2008), and their morphologies are similar to calcite crystals that form in laboratory experiments when ACC precipitates from highly supersaturated solutions and crystallizes to calcite via spherulitic growth (e.g., Fig. 5.3a).

Two main factors explain the different crystallization pathways of ACC to either primary vaterite or calcite. The first one relates the structure of ACC and its formation mechanisms and pathways. Gebauer et al. (2008) suggested that the binding strength of Ca^{2+} and $CO_3{}^{2-}$ ions within the ACC precursor clusters is pH-dependent and controls the structure, stability, and crystallization pathways of ACC. This way, ACC formed at a basic pH has a vaterite-type local structure and promotes the crystallization of vaterite over calcite, while ACC formed at a neutral pH has a calcite-type local structure and crystallizes directly to calcite. The second factor relates pH, solubility, and the dissolution rate of ACC (Kojima et al. 1993). The solubility (and dissolution rate) of ACC increase proportionally with formation pH, and thus, the saturation index for any anhydrous crystalline carbonate when an aqueous solution is in equilibrium with respect to ACC will be directly proportional to the pH at which ACC formed. Taking all this together, an ACC precursor formed at high pH does not only have a vaterite-type local structure but also promotes the crystallization of vaterite because of its higher solubility and dissolution rate. Conversely, ACC formed at a starting neutral pH has a calcite-type local structure and also a lower solubility so it tends to transform directly to calcite (Demichelis et al. 2011; Raiteri et al. 2012; Gebauer et al. 2014; also see Chap. 6 by Demichelis et al. 2017 in this book).

It is very important to take into account that ACC formation is extremely fast (<0.1 s), even at low supersaturation levels. This is critical for most experimental methods used for calcium carbonate crystallization and in particular when solution mixing-based methods are used (as opposed to slow diffusion methods). As ACC is forming during fast mixing, it is experimentally challenging to avoid local differences in the mixed solution and thus local ACC formation regardless how rapid or homogeneous mixing can be achieved. For example, when a $CaCl_2$ solution is added to a Na_2CO_3 solution, the first ACC nanoparticles form in a higher pH environment compared to those ones forming at the end of the mixing procedure. This means that during the mixing procedure, we have a changing pH that affects the short-range structure and chemical composition of any forming ACC (e.g., hydration, incorporation of OH^- ions). As a result, ACC nanoparticles with different short-range structures (vaterite and calcite type) can coexist in the same experiment/sample. This naturally downstream during the crystallization process can also result in a mixture of vaterite and calcite (Zou et al. 2015). There are other parameters that can also affect strongly the outcome of mixing experiments; these include temperature, concentrations/supersaturation levels of the starting solutions, aqueous $Ca^{2+}/CO_3{}^{2-}$ ratios, pH of the final solution once equilibrium with respect to ACC has been reached, stirring/shaking rate, additives, etc. In addition, the particle size of ACC is inversely proportional to the initial supersaturation, and this needs to be taken into account because the solubility of nanoparticles is inversely proportionally with the particle size (e.g., Hochella et al. 2008). Considering this large number of variables, it is not surprising to find experimental reproducibility problems during synthesis of crystalline $CaCO_3$ polymorphs at high supersaturations. In fact, some variables that seem to be negligible or difficult to control, like mixing procedure, stirring rate or small variations in the concentrations of the starting solutions, are actually significant enough to affect the short-range structure, dissolution kinetics, and crystallization pathways of ACC (e.g., Zou et al. 2015; Ševčík et al. 2015).

5.3 The Effect of (In)organics in the Formation of ACC and Vaterite

A wide range of industrial, medical, and pharmaceutical applications rely on simple protocols to produce $CaCO_3$ phases in a way that they can have a high degree of control over the resulting polymorph type and morphology. Organisms are experts in this field, and it is well known that the formation of calcium carbonates most often proceeds in the presence of, or through templating on, simple inorganic/complex organic molecules. This leads to elaborate morphologies and textures that could have innumerable applications (e.g., Trushina et al. 2014) in industry if we were able to reproduce them. Over the past decades, researchers have taken inspiration from biomineralizing organisms and employed a range of organic and inorganic compounds aiming to mimic their strategies and achieve control over morphology, textures, composition, and shapes of biomimetic $CaCO_3$ phases (e.g., Kim et al. 2011; Schenk et al. 2014a, b). This is not easy because the diversity of possible compounds that could be used as additives or templating agents span from simple ions such as Mg^{2+}, Sr^{2+}, REE^{3+}, $SO_4{}^{2-}$, $PO_4{}^{3-}$, and $SiO_4{}^{2-}$ to a suite of organic molecules including (poly)carboxylates, cationic and anionic polyelectrolytes, amino acids, (block) copolymers, surfactants, proteins, polysaccharides, phosphate compounds (e.g., phosphoenolpyruvate), dendrimers, and alcohols (Meldrum and Cölfen 2008 and references therein).

The effects of (in)organic compounds on the formation of ACC and its crystallization to vaterite are primarily linked to variations in ACC lifetime, vaterite morphologies, and particle size. As explained above, these are usually coupled to variations in formation and crystallization mechanisms and pathways. Changes in vaterite morphology are quite common, both when it crystallizes as a single crystal (e.g., development of preferred crystal faces; Hu et al. 2012) or when it forms aggregates of nanoparticles (e.g., variation in angle of branching of spherulites, formation of hollow spheres; Cai et al. 2008; Beck and Andreassen 2010). The detailed outcome of such reactions varies greatly with the complexity and concentrations of additive, variations in starting and end solution compositions, and the experimental method used. The effects that (in)organic additives have on ACC to vaterite transformations also depend on density and chemistry of the functional groups in a polymer molecule but also a range of other factors such as their structure, chain length, hydrophobicity, or conformation. Provided a sufficient amount of an (in)organic additive is present, the lifetime of ACC and/or vaterite is usually prolonged, either by stabilization via a protective organic coating (Gal et al. 2013), inhibiting the formation of crystalline phases (e.g., Mg^{2+} unstabilizes the structure of vaterite; Rodriguez-Blanco et al. 2012) and/or incorporation of the additives which slow down the dehydration of ACC during its transformation (Rodriguez-Blanco et al. 2014; Rodriguez-Blanco et al. 2015).

Inorganic additives are usually incorporated into both ACC and vaterite. However, the incorporation of inorganic cations or anions into a crystalline $CaCO_3$ polymorph is favored or inhibited depending on its structure. For example, tetrahedral anions such as $SiO_4{}^{2-}$ and $PO_4{}^{3-}$ do not fit well into the calcite structure, and their presence results in the stabilization of ACC and vaterite but the inhibition of their transformation to calcite (Gal et al. 2010). Most of the studies about inorganic additives on carbonate formation pathways or stability have focused on the effects of Mg^{2+} and $SO_4{}^{2-}$ ions, as they are most abundant divalent ions in our oceans and because they are considered to control the primary inorganic marine calcium carbonate mineralogy throughout the Phanerozoic (Bots et al. 2011). On the other hand, sulfate slows down the rate of vaterite formation and particle growth (transformation of ACC to vaterite is $\sim 10\,\%$ slower than in the pure system), but most importantly, the presence of sulfate stabilizes vaterite (Bots et al. 2012). The effect of Mg^{2+} on the mechanism of ACC and vaterite formation is remarkable: Mg^{2+} gets incorporated in ACC and calcite, but the vaterite structure becomes unstable at higher Mg^{2+} concentrations (Bots et al. 2012). Mg^{2+} ions have a higher dehydration energy compared to Ca^{2+} (Di Tommaso and de Leeuw 2010), and hence, the presence of Mg^{2+} in ACC affects its dehydration prior to crystallization and reduces its dissolution rate. A slower rate of dissolution is translated into a slower increase of the solution supersaturation, influencing the crystallization pathways. In contrast to pure ACC, which directly crystallizes to vaterite or calcite (Rodriguez-Blanco et al. 2011), an increasing content of Mg^{2+} in ACC increases its stability and promotes the crystallization of Mg-calcite ($10\,\%$ Mg^{2+}; Rodriguez-Blanco et al. 2012), monohydrocalcite ($30\,\%$ Mg^{2+}; Rodriguez-Blanco et al. 2014), and dolomite ($50\,\%$ Mg^{2+}; Rodriguez-Blanco et al. 2015). In particular, the crystallization of dolomite from Mg-bearing ACC requires high temperatures ($> 60°$ C) because of the larger energy needed to dehydrate ACC with a high Mg content ($Ca_{0.606}Mg_{0.394}CO_3 \cdot 1.37H_2O$; Rodriguez-Blanco et al. 2015). After a temperature-dependent induction time, Mg-ACC partially dehydrates and orders prior to its rapid (<5 min) crystallization to nonstoichiometric proto-dolomite via spherulitic growth. Proto-dolomite has no ordering of Mg^{2+} and Ca^{2+} within its structure and transforms to highly crystalline and stoichiometric dolomite on a much longer timescale (hours to days), via an Ostwald-ripening mechanism (Malone et al. 1996). This crystallization route is completely different to the well-known dolomitization of calcite (secondary replacement of Mg^{2+} into previously precipitated calcite; e.g., Sibley et al. 1994) and is an excellent example of how inorganic ions can affect the crystallization pathways of carbonates and the stability and solubility of ACC.

In the case of organic additives, anionic groups have been proved important for ACC and vaterite stabilization in solution (Naka et al. 2006; Olderoy et al. 2009; Gal et al. 2010; Boyjoo et al. 2014; Tobler et al. 2014; Tobler et al. 2015). Some organics have given particularly interesting results, like polyacrylic acid (PAA; Xu et al. 2008) and polymerized dopamine (Wang and Xu 2013), stabilizing ACC up to half a month in solution and more than a year in dry conditions, respectively. In the case of vaterite, peptide block copolymers are able to inhibit the vaterite–calcite transformation at least a year (Kašparová et al. 2004). In most cases, the majority of the organic additives are adsorbed on the surface of the nanoparticles, so their lifetimes are proportional to the concentration of additive. This coating is thought to prevent particle aggregation and recrystallization by limiting diffusion (Gal et al. 2013) or by making them less soluble (Gal et al. 2014). Incorporation, and an associated change in the short-range structure of ACC particles, has been reported for citrate (Tobler et al. 2015). However, for amino acids such as glycine and aspartic acid, ACC was also stabilized, but incorporation was not observed at comparable concentrations (Tobler et al. 2014). Organic compounds have also been reported to change the crystallization mechanism of vaterite. The resulting change in solution chemistry with additive addition plays a large role for the fate of ACC and vaterite. Polymers with anionic groups can complex free calcium ions in solution, serving as nucleation points with decreased barriers for nucleation and also resulting into a change in supersaturation and promoting a change in particle size. A lower supersaturation results in lower nucleation density compared to a system with a higher supersaturation. Naka et al. (2006) studied cross sections of vaterite formed in the presence of PAA finding out that at high concentrations, the formation of vaterite occurred via an aggregation process. However, at low initial concentration, or when PAA was added later to the reaction, radial growth characteristic for spherulitic growth was observed. Olderoy et al. (2009) performed experiments at the same initial supersaturation and pH of $\sim$7 and found that alginate enhanced nucleation but inhibited growth and aggregation, resulting in a large number of small vaterite nanoparticles with no other significant change in morphology.

The vaterite morphology is particularly sensitive to changes in solution chemistry, and a wide range of shapes have been reported in the presence of additives. These shapes include dumbbells, disks, spheres, flowers, and flakes. A comprehensive overview is presented in Boyjoo et al. (2014) along with solution pH, method, additive, and concentration. They found that solution pH has a drastic effect on vaterite morphology but not on polymorphism. Addition of organic molecules can also cause a change in pH, which affects speciation, the degree of protonation of the added molecule, and the supersaturation levels. Decreased water activity also has a significant impact on stability, morphology, and polymorph selection of $CaCO_3$. By adding 10 and 50 % of short alcohol molecules, we (Sand et al. 2012) (Fig. 5.4) stabilized amorphous and crystalline phases and were able to change the

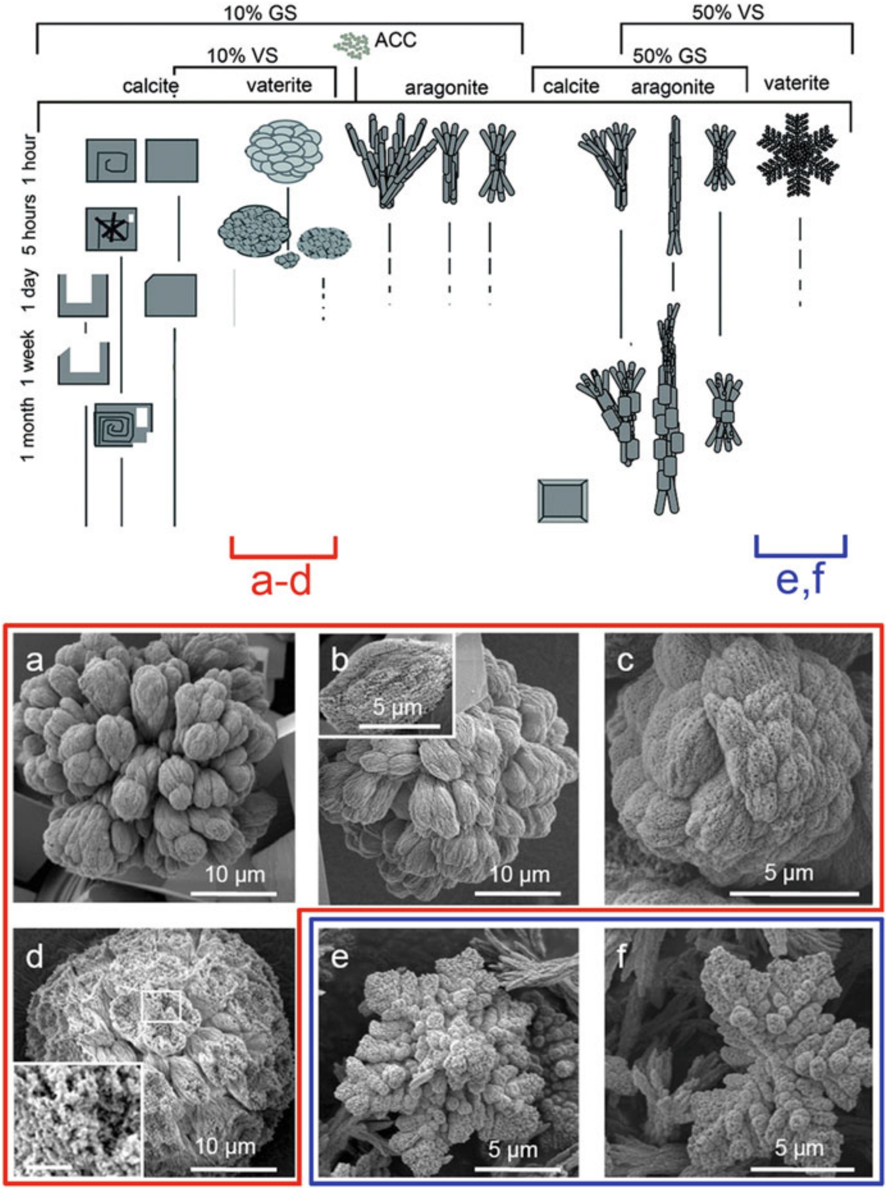

Fig. 5.4 *Top* diagram shows the morphological evolution of calcite, vaterite, and aragonite over time for various experimental regimes in ethanol-rich solutions (10 and 50 % ethanol; GS and VS refer to gentle shaking and vigorous shaking conditions, respectively). SEM images below represent the morphology for vaterite obtained from experiments with 10 and 50 % ethanol. With 10 % alcohol, the morphologies are independent of shaking speed (**a**–**d**): (**a**, **b**) cauliflower and layer cake (*inset* in **b**) crystals form in the GS regime after 1 h. Calcite crystals are often attached to the vaterite clusters, as seen in **a** and **b**; (**c**) VS regime after 1 h showing more porous vaterite cauliflower structures; (**d**) during the vaterite to calcite transformation, the cauliflower spheres become corroded (the *scale bar* in *inset* is 1 µm); (**e**, **f**) dendritic vaterite precipitated in the VS experiments with 50 % alcohol and sampled after 5 h; aragonite needles are present in both images (Adapted after Sand et al. 2012)

crystallization pathway by varying the shaking speed. These effects became more pronounced with a higher alcohol/water ratio: at 50 % alcohol, vaterite only formed at high shaking speeds, and it was still stable after a day in contrast to the 5–6 h of lifetime in the pure system at ambient temperature. We explained this stabilizing effect by the lower water activity due to decreased reaction kinetics and by the adsorption of the alcohol molecules. The latter creates a hydrophobic adsorption layer toward the bulk liquid decreasing the ion transport between solid and solution (Sand et al. 2010).

Despite the fact that organic additives can influence the final morphology by adsorbing to active growth sites or by changing the local ion transport pathway, it is also necessary to highlight that organic additives have a great influence on the kinetics of ACC dissolution. Because of the relatively similar solubility products of vaterite, aragonite, and calcite, the kinetics of dissolution of ACC can result in different supersaturation levels, promoting the formation of one or other $CaCO_3$ polymorphs.

5.4 Outlook

In the chapter above, we summarized the state of knowledge about how the transformation of amorphous calcium carbonate to crystalline $CaCO_3$ polymorphs proceeds in the presence, or absence, of important inorganic and organic additives in nature and in biomimetic systems. Although, as described, much research has been done to address these issues, there are still several open questions that we want to highlight as future research goals:

- Can aragonite crystallize directly from ACC with no other intermediate $CaCO_3$ polymorph affecting the reaction? Data about the pathways that lead to the formation of several other aragonite-like minerals (e.g., strontianite ($SrCO_3$) or whiterite ($BaCO_3$)) have suggested that a direct crystallization from solution of these carbonate phases may be feasible. However, the available data are still sketchy, and it is still unclear if in these systems, an amorphous precursor was not present or if there was an amorphous precursor present which was too short-lived to be detected.
- Why are there seemingly multiple "vaterite" structures and what drives the observed differences? It may be that the nanocrystalline nature of vaterite and its propensity to "sequester" some ions more easily than others may be the prime reason for the observed differences in structure. Yet, the fundamental mechanistic reasons for these differences are still unclear. The questions related to which (in)organic molecules affect the formation/aggregation/transformation of vaterite more than others and if, and how, such molecules become "incorporated" into the vaterite structure or if they just lead to defects is still debated and requires further research.

- Finally the bigger picture question! It is well known that the nature and stability (or not) of ACC and vaterite as precursors and/or intermediates to crystalline $CaCO_3$ polymorphs are crucial for many global biogeochemical cycles as well as many industrial processes. However, the complexity of the $CaCO_3$ system has so far prevented us from establishing a “unified” crystallization model. In natural settings, a chemically pure system does not exist, and the presence of (in)organic compounds, together with variations in physicochemical parameters, invariably affects the kinetics and mechanisms of crystallization. However, an elegant and simple model for ACC crystallization would improve, for example, our ability to design better biomimetic reactions and thus more efficient industrial processes. Equally, a “unified” model of $CaCO_3$ crystallization would also allow us to better predict the effects that, for example, changes in ocean chemistry due to climate change, have on the stability and formation of calcium carbonate shells in marine biota, which control to a large extent our global carbon cycle. Despite all the efforts done so far, it is clear that we are still at the beginning of an exciting research endeavor that will keep several generations of geochemists and chemists busy.

Acknowledgments J.D. Rodriguez-Blanco would like to acknowledge the EU-funded NanoCArB Marie Curie Intra-European Fellowship (IEF) under contract PIEF-GA-2013-624016. K.K. Sand is grateful for funding from the Danish Council for Independent Research on their Individual Post Docs (0602-02915B) and Sapere Aude program (0602-02654B) and support from the US Department of Energy, Office of Basic Energy Sciences, Division of Chemical Sciences, Geosciences, and Biosciences at Pacific Northwest National Laboratory, which is operated by Battelle for the US Department of Energy under Contract DE-AC05-76RL01830.

References

Ahmed IAM, Benning LG, Kakonyi G, Sumoondur A, Terrill N, Shaw S (2010) The formation of green rust sulfate: in situ and time-resolved scattering and electrochemistry. Langmuir 26:6593–6603

Andreassen JP, Flaten EM, Beck R, Lewis AE (2010) Investigations of spherulitic growth in industrial crystallization. Chem Eng Res Des 88:1163–1168

Beck R, Andreassen JP (2010) Spherulitic growth of calcium carbonate. Cryst Growth Des 10:2934–2947

Beniash E, Aizenberg J, Addadi L, Weiner S (1997) Amorphous calcium carbonate transforms into calcite during sea urchin larval spicule growth. Proc R Soc Lond Ser B 264:461–465

Bots P, Benning LG, Rickaby REM, Shaw S (2011) The role of SO4 in the switch from calcite to aragonite seas. Geology 39:331–334

Bots P, Benning LG, Rodriguez-Blanco JD, Roncal-Herrero T, Shaw W (2012) Mechanistic insights into the crystallization of amorphous calcium carbonate (ACC). Cryst Growth Des 12:3806–3814

Boyjoo Y, Pareek VK, Liu J (2014) Synthesis of micro and nano-sized calcium carbonate particles and their applications. J Mater Chem A 2:14270–14288

Brinza L, Schofield PF, Hodson ME, Weller S, Ignatyev K, Geraki K, Quinn PD, Mosselmans JFW (2014) Combining μXANES and μXRD mapping to analyse the heterogeneity in calcium carbonate granules excreted by the earthworm Lumbricus terrestris. J Synchrotron Radiat 21:235–241

Brinza L, Vu HP, Shaw S, Mosselmans FJ, Benning LG (2015) Effect of Mo and V on the hydrothermal crystallization of hematite from ferrihydrite: an in situ energy dispersive X-Ray diffraction and X-Ray absorption spectroscopy study. Cryst Growth Des 15:768–4780

Briones MJI, López E, Méndez J, Rodríguez JB, Gago-Duport L (2008) Biological control over the formation and storage of amorphous calcium carbonate by earthworms. Mineral Mag 72:227–231

Burke IT, Mosselmans FW, Shaw S, Peacock CL, Benning LG, Cocker VS (2015) Impact of the diamond light source on research in earth and environmental sciences: current work and future perspectives. In: Materlik G, Stuart D, Rayment T (eds) Research achieved with diamond and future perspectives. Philos Trans A 373:20130151

Cahill CL, Benning LG, Barnes HL, Parise JB (2000) In situ time-resolved X-ray diffraction of iron sulfides during hydrothermal pyrite growth. Chem Geol 167:53–63

Cai A, Xu X, Pan H, Tao J, Liu R, Tang R, Cho K (2008) Direct synthesis of hollow vaterite nanospheres from amorphous calcium carbonate nanoparticles via phase transformation. J Phys Chem C 112:11324–11330

Canti MG, Piearce TG (2003) Morphology and dynamics of calcium carbonate granules produced by different earthworm species. Pedobiologia 47:511–521

Davidson LE, Shaw S, Benning LG (2008) The kinetics and mechanisms of schwertmannite transformation to goethite and hematite under alkaline conditions. Am Mineral 93:1326–1337

Demichelis R, Raiteri P, Gale JD, Quigley D, Gebauer D (2011) Stable prenucleation mineral clusters are liquid-like ionic polymers. Nat Commun 2:590

Demichelis R, Raiteri P, Gale JD (2017) Ab Initio modelling of the structure and properties of crystalline calcium carbonate. In: Van Driessche AES, Kellermeier M, Benning LG, Gebauer D (eds) New perspectives on mineral nucleation and growth, Springer, Cham, pp 113–136

Di Tommaso D, De Leeuw NH (2010) Structure and dynamics of the hydrated magnesium ion and of the solvated magnesium carbonates: insights from first principles simulations. Phys Chem Chem Phys 12:894–901

Dove PM, De Yoreo JJ, Weiner S (eds) (2003) Reviews in mineralogy and geochemistry, vol 154. Mineralogical Society of America, Chantilly

Faatz M, Gröhn F, Wegner G (2004) Amorphous calcium carbonate: synthesis and potential intermediate in biomineralization. Adv Mater 16:996–1000

Fedorov PP, Nazarkin MV, Zakalyukin RM (2002) On polymorphism and morphotropism of rare earth sesquioxides. Crystallogr Rep 47:281–286

Foran E, Weiner S, Fine M (2013) Biogenic fish-gut calcium carbonate is a stable amorphous phase in the gilt-head seabream sparus aurata. Sci Rep 3:1700

Fujiwara M, Shiokawa K, Araki M, Ashitaka N, Morigaki K, Kubota T, Nakahara Y (2010) Encapsulation of proteins into $CaCO_3$ by phase transition from vaterite to calcite. Cryst Growth Des 10:4030–4037

Gago-Duport L, Briones MJ, Rodríguez JB, Covelo B (2008) Amorphous calcium carbonate biomineralization in the earthworm's calciferous gland: pathways to the formation of crystalline phases. J Struct Biol 162:422–435

Gal A, Weiner S, Addadi L (2010) The stabilizing effect of silicate on biogenic and synthetic amorphous calcium carbonate. J Am Chem Soc 132:13208–13211

Gal A, Hirsch A, Siegel S, Li C, Aichmayer B, Politi Y, Fratzl P, Weiner S, Addadi L (2012) Plant cystoliths: a complex functional biocomposite of four distinct silica and amorphous calcium carbonate phases. Chemistry 18:10262–10270

Gal A, Habraken W, Gur D, Fratzl P, Weiner S, Addadi L (2013) Calcite crystal growth by a solid-state transformation of stabilized amorphous calcium carbonate nanospheres in a hydrogel. Angew Chem Int Ed 52:4867–4870

Gal A, Kahil K, Vidavsky N, DeVol RT, Gilbert PUPA, Fratzl P, Weiner S, Addadi L (2014) Particle accretion mechanism underlies biological crystal growth from an amorphous precursor phase. Adv Funct Mater 24:5420–5426

Gebauer D, Völkel A, Cölfen H (2008) Stable prenucleation calcium carbonate clusters. Science 322:819–1822

Gebauer D, Kellermeier M, Gale JD, Bergström L, Cölfen H (2014) Pre-nucleation clusters as solute precursors in crystallisation. Chem Soc Rev 43:2348–2371

Gong YUT, Killian CE, Olson IC, Appathurai NP, Amasino AL, Martin MC, Holt LJ, Wilt FH, Gilbert PUPA (2012) Phase transitions in biogenic amorphous calcium carbonate. Proc Natl Acad Sci U S A 109:6088–6093

Goodwin AL, Michel FM, Phillips BL, Keen DA, Dove MT, Reeder RJ (2010) Nanoporous structure and medium-range order in synthetic amorphous calcium carbonate. Chem Mater 22:3197–3205

Gránásy L, Pusztai T, Tegze G, Warren JA, Douglas JF (2005) Growth and form of spherulites. Phys Rev E 72:011605

Hochella MF, Lower SK, Maurice PA, Penn RL, Sahai N, Sparks DL, Twining BS (2008) Nanominerals mineral nanoparticles and earth systems. Science 319:1631–1635

Hodson ME, Benning LG, Demarchi B, Penkman KEH, Rodriguez-Blanco JD, Schofield PF, Versteegh EAA (2015) Biomineralisation by earthworms – an investigation into the stability and distribution of amorphous calcium carbonate. Geochem Trans 16:4

Holcomb M, Cohen AL, Gabitov RI, Hutter JL (2009) Compositional and morphological features of aragonite precipitated experimentally from seawater and biogenically by corals. Geochim Cosmochim Acta 73:4166–4179

Hu Q, Zhang J, Teng H, Becker U (2012) Growth process and crystallographic properties of ammonia-induced vaterite. Am Mineral 97:1437–1445

Isaure MP, Sarret G, Harada E, Choi YE, Marcus MA, Fakra SC, Geoffroy N, Pairis S, Susini J, Clemens S, Manceau A (2010) Calcium promotes cadmium elimination as vaterite grains by tobacco trichomes. Geochim Cosmochim Acta 74:5817

Kabalah-Amitai L, Mayzel B, Kauffmann Y, Fitch AN, Bloch L, Gilbert PUPA, Pokroy B (2013) Vaterite crystals contain two interspersed crystal structures. Science 340:454–457

Kašparová P, Antonietti M, Cölfen H (2004) Double hydrophilic block copolymers with switchable secondary structure as additives for crystallization control. Colloids Surf A Physicochem Eng Asp 250:153–162

Kim YY, Hetherington NB, Noel EH, Kröger R, Charnock JM, Christenson HK, Meldrum FC (2011) Capillarity creates single-crystal calcite nanowires from amorphous calcium carbonate. Angew Chem Int Ed Engl 50:12572–12577

Kojima Y, Kawanobe A, Yasue T, Arai Y (1993) Synthesis of amorphous calcium carbonate and its crystallization. J Ceram Soc Jpn 101:1145–1152

Lowenstam HA, Abbott DP (1975) Vaterite: a mineralization product of the hard tissues of a marine organism (Ascidiacea). Science 188:363–365

Malone JM, Baker PA, Burns SJ (1996) Recrystallization of dolomite: an experimental study from 50–200°C. Geochim Cosmochim Acta 60:2189–2207

Meldrum FC, Cölfen H (2008) Controlling mineral morphologies and structures in biological and synthetic systems. Chem Rev 108:4332–4432

Naka K, Huang Y, Chujo Y (2006) Formation of stable vaterite with poly(acrylic acid) by the delayed addition method. Langmuir 22:7760–7767

Nielsen MH, Aloni S, De Yoreo JJ (2014) In situ TEM imaging of $CaCO_3$ nucleation reveals coexistence of direct and indirect pathways. Science 345:1158–1162

Ogino T, Suzuki T, Sawada K (1987) The formation and transformation mechanism of calcium carbonate in water. Geochim Cosmochim Acta 51:2757–2767

Olderoy MO, Xie ML, Strand BL, Flaten EM, Sikorski P, Andreassen JP (2009) Growth and nucleation of calcium carbonate vaterite crystals in presence of alginate. Cryst Growth Des 9:5176–5183

Parakhonskiy BV, Haase A, Antolini R (2012) Sub-micrometer vaterite containers: synthesis substance loading and release. Angew Chem Int 51:1195–1197

Politi Y, Metzler RA, Abrecht M, Gilbert B, Wilt FH, Sagi I, Addadi L, Weiner S, Gilbert PUPA (2008) Transformation mechanism of amorphous calcium carbonate into calcite in the Sea urchin larval spicule. Proc Natl Acad Sci U S A 105:20045–20045

Pouget EM, Bomans PHH, Goos JACM, Frederik PM, With G, Sommerdijk NAJM (2009) The initial stages of template-controlled CaCO3 formation revealed by cryo-TEM. Science 323:1455–1458

Pouget EM, Bomans PHH, Dey A, Frederik PM, de With G, Sommerdijk NAJM (2010) The development of morphology and structure in hexagonal vaterite. J Am Chem Soc 132:11560–11565

Qiao L, Feng QL, Li Z (2007) Special vaterite found in freshwater lackluster pearls. Cryst Growth Des 7:275–279

Radha AV, Forbes TZ, Killian CE, Gilbert PUPA, Navrotsky A (2010) Transformation and crystallization energetics of synthetic and biogenic amorphous calcium carbonate. Proc Natl Acad Sci U S A 107:16438–16443

Raiteri P, Demichelis R, Gale JD, Kellermeier M, Gebauer D, Quigley D, Wright LB, Walsh TR (2012) Exploring the influence of organic species on pre-and post-nucleation calcium carbonate. Faraday Discuss 1:61–85

Rodriguez-Blanco JD, Shaw S, Benning LG (2008) How to make ‘stable’ ACC: protocol and preliminary structural characterization. Mineral Mag 72:283–286

Rodriguez-Blanco JD, Shaw S, Benning LG (2011) The kinetics and mechanisms of amorphous calcium carbonate (ACC) crystallization to calcite via vaterite. Nanoscale 3:265–271

Rodriguez-Blanco JD, Shaw S, Bots P, Roncal-Herrero T, Benning LG (2012) The role of pH and Mg on the stability and crystallization of amorphous calcium carbonate. J Alloys Compd 536:S477–S479

Rodriguez-Blanco JD, Shaw S, Bots P, Roncal-Herrero T, Benning LG (2014) The role of Mg in the crystallisation of monohydrocalcite. Geochim Cosmochim Acta 127:204–220

Rodriguez-Blanco JD, Shaw S, Benning LG (2015) A route for the direct crystallization of dolomite. Am Mineral 100:1172–1181

Rowlands DLG, Webster RK (1971) Precipitation of vaterite in lake water. Nat Phys Sci 229:158

Sánchez-Román M, McKenzie JA, Wagener ALR, Romanek CS, Sánchez-Navas A, Vasconcelos C (2011) Experimentally determined biomediated Sr partition coefficient for dolomite: significance and implication for natural dolomite. Geochim Cosmochim Acta 75:887–904

Sand KK, Yang M, Makovicky E, Cooke DJ, Hassenkam T, Bechgaard K, Stipp SLS (2010) Binding of ethanol on calcite: the role of the OH bond and its relevance to biomineralization. Langmuir 26:15239–15247

Sand KK, Rodriquez-Blanco JD, Makovicky E, Benning LG, Stipp SLS (2012) Crystallization of CaCO3 in water-alcohol mixtures: spherulitic growth polymorph stabilization and morphology change. Cryst Growth Des 12:845–853

Schenk AS, Albarracin EJ, Kim YY, Ihli J, Meldrum FC (2014a) Confinement stabilises single crystal vaterite rods. Chem Commun 50:4729–4732

Schenk AS, Cantaert B, Kim YY, Li Y, Read ES, Semsarilar M, Armes SP, Meldrum FC (2014b) Systematic study of the effects of polyamines on calcium carbonate precipitation. Chem Mater 26:2703–2711

Ševčík R, Pérez-Estébanez M, Viani A, Šašek P, Mácová P (2015) Characterization of vaterite synthesized at various temperatures and stirring velocities without use of additives. Powder Technol 284:265–271

Shen Q, Wei H, Zhou Y, Huang Y, Yang H, Wang D, Xu D (2006) Properties of amorphous calcium carbonate and the template action of vaterite spheres. J Phys Chem B 110:2994–3000

Shtukenberg AG, Punin YO, Gunn E, Kahr B (2012) Spherulites. Chem Rev 112:1805–1838

Sibley DF, Nordeng SH, Borkowski ML (1994) Dolomitization kinetics in hydrothermal bombs and natural settings. J Sediment Res 64:630–637

Tobler DJ, Benning LG (2011) The microbial diversity in Icelandic hot springs: temperature salinity pH and sinter growth rate effects. Extremophiles 15:473–485

Tobler DJ, Shaw S, Benning LG (2009) Quantification of initial steps of nucleation and growth of silica nanoparticles: an in-situ SAXS and DLS study. Geochim Cosmochim Acta 73:5377–5393

Tobler DJ, Rodriguez-Blanco JD, Dideriksen K, Sand KK, Bovet N, Benning LG, Stipp SLS (2014) Effect of aspartic acid and glycine on amorphous calcium carbonate (ACC) structure stability and crystallisation. Procedia Earth Planet Sci 10:143–148

Tobler DJ, Rodriguez-Blanco JD, Dideriksen K, Sand KK, Bovet N, Benning LG, Stipp SLS (2015) Citrate effects on amorphous calcium carbonate (ACC) structure stability and crystallization. Adv Funct Mater 25:3081–3090

Tobler DJ, Rodriguez-Blanco JD, Sørensen HO, Stipp SLS, Dideriksen K (2016) Effect of pH on amorphous calcium carbonate structure and transformation. Cryst Growth Des 16:4500–4508

Trushina D, Bukreeva TV, Kovalchuk MV, Antipina MN (2014) $CaCO_3$ vaterite microparticles for biomedical and personal care applications. Mater Sci Eng C 45:644–65

Vallina B, Rodriguez-Blanco JD, Blanco JA, Benning LG (2014) The effect of heating on the morphology of crystalline neodymium hydroxycarbonate NdCO3OH. Mineral Mag 78:1391–1397

Vallina B, Rodriguez-Blanco JD, Brown AP, Blanco JA, Benning LG (2015) The role of amorphous precursors in the crystallization of La and Nd carbonates. Nanoscale 7:12166–12179

Vu HP, Shaw S, Brinza L, Benning LG (2010) Crystallization of hematite (alpha-Fe_2O_3) under alkaline condition: the effects of Pb. Cryst Growth Des 10:1544–1551

Wang J, Becker U (2012) Energetics and kinetics of carbonate orientational ordering in vaterite calcium carbonate. Am Mineral 97:1427–1436

Wang SS, Xu AW (2013) Amorphous calcium carbonate stabilized by a flexible biomimetic polymer inspired by marine mussels. Cryst Growth Des 13:1937–1942

Wang D, Wallace AF, De Yoreo JJ, Dove PM (2009) Carboxylated molecules regulate magnesium content of amorphous calcium carbonates during calcification. Proc Natl Acad Sci U S A 106:21511–21516

Warthmann R, van Lith Y, Vasconcelos C, McKenzie JA, Karpoff AM (2000) Bacterially induced dolomite precipitation in anoxic culture experiments. Geology 28:1091–1094

Wehrmeister U, Jacob DE, Soldati AL, Loges N, Häger T, Hofmeister W (2011) Amorphous nanocrystalline and crystalline calcium carbonates in biological materials. J Raman Spectrosc 42:926–935

Xu XR, Cai AH, Liu R, Pan HH, Tang RK, Cho KW (2008) The roles of water and polyelectrolytes in the phase transformation of amorphous calcium carbonate. J Cryst Growth 310:3779–3787

Zou Z, Bertinetti L, Politi Y, Jensen ACS, Weiner S, Addadi L, Fratzl P, Habraken WJEM (2015) Opposite particle size effect on amorphous calcium carbonate crystallization in water and during heating in air. Chem Mater 27:4237–4246